Greek Letters

α = heat transfer coefficient
β = mass transfer coefficient
$(-\Delta H_R)$ = reaction enthalpy
ϵ = part of free space in the fixed bed
$(\rho c_p)_F$ = heat capacity of the fluid
$(\rho c_p)_S$ = heat capacity of the catalyst
$\xi = c_{AX}/c_{Xo}$ = dimensionless concentration of the chemisorbed species A

LITERATURE CITED

Eigenberger, G., "Mechanismen und Auswirkungen kinetischer Instabilitäten bei heterogen-katalytischen Reaktionen," Habilitationsschrift, Universität Stuttgart, West Germany (1976).

Fieguth, P., and E. Wicke, "Der Übergang vom Zünd-/Lösch-Verhalten zu stabilen Reaktionszuständen bei einem adiabatischen Rohrreaktor," *Chem. Ing. Techn.*, 43, 604 (1971).

Frank, U. F., "Chemische Oszillationen," *Angewandte Chemie*, 1, 1 (1978).

Gilles, E. D., "Reactor Models, Fourth International Symposium on Chemical Engineering," Heidelberg (1976).

———, G. Eigenberger, and W. Ruppel, "Relaxation Oscillations in Chemical Reactors," paper presented at AIChE Meeting, Chicago, Ill. (1976).

Horák, J., and F. Jirácek, "A study of the dynamic behaviour of catalytic flow reactors," II. Int. Symp. Chem. Reaction Engng. Amsterdam, B8-1, Elsevier (1972).

Lübeck, B., "Kontinuierliche Modelle katalytischer Festbettreaktoren und ihre digitale Simulation mit Integralgleichungen," Dissertation, Universität Stuttgart, West Germany (1975).

Ruppel, W., and M. Zeitz, "Implicit Simulation Method for Distributed Parameter Systems on a Hybrid Computer," *Proc. Intern. Assoc. Analog Computation*, 3, 1 (1975).

Sheintuch, M., and R. A. Schmitz, "Oscillations in Catalytic Reactions," *Catal. Rev.-Sci. Eng.*, 15, 107 (1977).

Manuscript received September 12, 1977; revision received May 30, and accepted June 21, 1978.

Transient Gas-Liquid Flow in Horizontal Pipes: Modeling the Flow Pattern Transitions

The theory for predicting flow pattern transition under transient flow conditions is developed and compared with experiment. This work represents an extension of the methods presented by Taitel and Dukler (1976) for steady state flows. Under transient conditions, flow pattern transitions can take place at flow rates substantially different than would occur under steady flow conditions. In addition, flow patterns can appear which would not be expected for a slow change in flow rates along that same path. Methods are presented for predicting the flow rates at which flow pattern transitions will take place during flow transients. The method also reveals when spurious flow patterns will appear.

YEHUDAH TAITEL
NAUGAB LEE
and
A. E. DUKLER

University of Houston
Houston, Texas 77004

SCOPE

During a concurrent gas-liquid flow in horizontal pipes, a variety of flow patterns can exist. Each pattern results from the particular manner by which the liquid and gas distribute in the pipe. Most observers classify the variety of observed distributions into six patterns as shown in Figure 1 (Govier and Aziz, 1972; Hewitt and Hall-Taylor, 1970). Rates of transport of energy and mass between the two phases as well as between the individual phases and the wall vary greatly with flow pattern. Given the steady state flow rates of the two phases, the fluid properties and the tube size, a central task to those attempting to model the two phase transport process or to design two phase flow equipment is to predict the particular flow pattern which will exist and the flow rate pairs at which transition between flow patterns will be observed. Figure 2 is an example of a flow pattern map for steady air-water at low pressures in 2.0 to 3.0 cm diameter pipes. The locus of the flow rate pairs at which transition takes place are shown.

In many cases of industrial interest, the flow rates vary with time. Examples include start-up or shutdown of process equipment, changes in flow rates in response to changes in planned operating conditions, and emergencies such as rapid depressurization of equipment due to accident conditions. A case of particular importance is that of a nuclear reactor under conditions of a loss of coolant accident. It is often essential to be able to predict the flow regimes during the transient. If a very slow change is made from one flow rate pair to a second and the path crosses several transition curves (Figure 2), experience has shown that the flow pattern transitions take place at the same flow rates as would be expected for equilibrium or steady flow. However, the same result is not observed for rapid transients.

It is the objective of this work to model the process of flow pattern transition under transient flow conditions, to provide methods for predicting such transitions, and to test the result against experiment.

CONCLUSIONS AND SIGNIFICANCE

Under transient flow conditions, transition from one flow pattern to another can take place at substantially different flow rates than would be observed for steady state flows. This result is demonstrated in this work both from theory and experiment. For very slow changes in the flow rates along a path that crosses several transition boundaries, the sequence of flow patterns observed will be identical to that for steady state flow. However, when the path is traversed rapidly, not only will the transitions take place at different rates, but flow regimes not expected along the steady state path can appear. For example, in Figure 11, the line AA'A''B is the path expected during a very slow change in gas flow rate. The observed flow patterns would be smooth stratified, wavy stratified, and annular, and the gas rate at which each transition would take place is shown. However, for a very rapid change in gas rate, the path is shown to be AB'B''B'''B. The transitions take place at different flow rates. In additions, slug flow appears during the transient path.

The theory and methodology for predicting the transition conditions under transient flow are developed in detail.

During horizontal,, concurrent gas liquid flow in pipes, a variety of flow patterns can exist. Each pattern results from the particular manner by which the liquid and gas distribute in the pipe. Authors differ somewhat in the name they assign to each of the flow patterns; nevertheless, the differences are small and most agree on six flow regimes (Govier and Aziz, 1972; Hewitt and Hall-Taylor, 1970) as shown in Figure 1.

1. Stratified smooth flow: in this case the liquid flows at the bottom of the pipe with gas at the top, and the interface between them is smooth.
2. Stratified wavy flow: the liquid and gas are separated as above, but the interface is wavy.
3. Elongated bubble flow or plug flow: elongated gas bubbles located adjacent to the top part of the tube move downstream. They are separated by sections of continuous liquid.
4. Slug flow: liquid slugs separated by gas pockets move violently downstream. The slug may be aerated with distributed small bubbles at higher gas flow rates. The distinction between elongated bubble flow and slug flow is not well defined. Basically, both have the same general appearance, and the differences between them are based on the degree of agitation of the flow and the height of the liquid film between slugs.
5. Annular flow: annular flow takes place at high gas flow rates. The gas flows in the center of the pipe while the liquid flows as an annular. Because of gravity, this film is thicker at the bottom than at the top of the pipe. Annular flow can be visualized as developing from slug flow when the aeration in the slug becomes sufficiently high to form a continuous gas phase. It forms from a stratified liquid when the gas velocity is sufficiently high to spread around the pipe.
6. Dispersed bubble flow: for high liquid flow rates, the gas is dispersed in the form of small bubbles within a continuous liquid phase. Normally, the bubble density at the top will be somewhat higher than at the bottom of the pipe.

Given the steady state flow rates of the two phases, the fluid properties, and the tube size, a central task is to predict the flow pattern which will take place. In the past, flow maps have been used in which experimentally observed transition boundaries are plotted as functions of two flow parameters or two dimensionless groups. The cross hatched curves of Figure 2 show an example of a recent flow map given by Mandhane et al. (1974), using the superficial velocities of liquid u_L^s and gas u_G^s. Many other maps based primarily on experiment preceded the work by Mandhane et al. (see, for example, Baker, 1954; Govier and Omer, 1962; Kosterin, 1949; Alves, 1954; Bergelin and Gazley, 1949; Hoogendoorn and Buitelaar, 1961; Johnson and Abou-Sabe, 1952; Sternling, 1965; Schicht, 1969; Al-Sheikh et al., 1970).

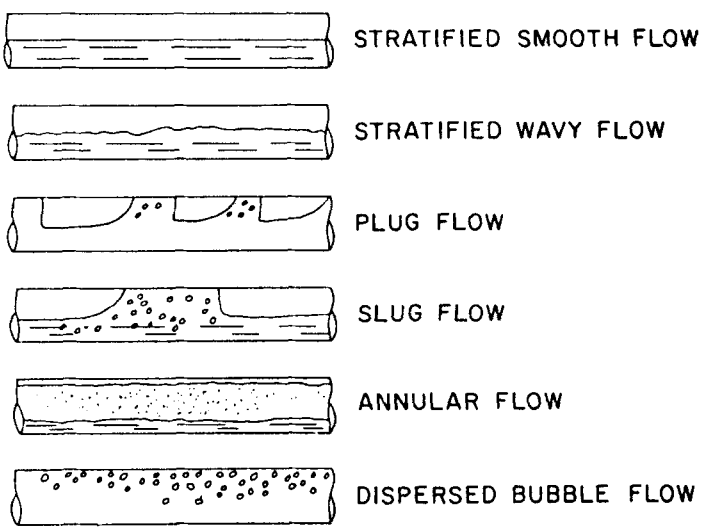

Fig. 1. Flow patterns in horizontal flow.

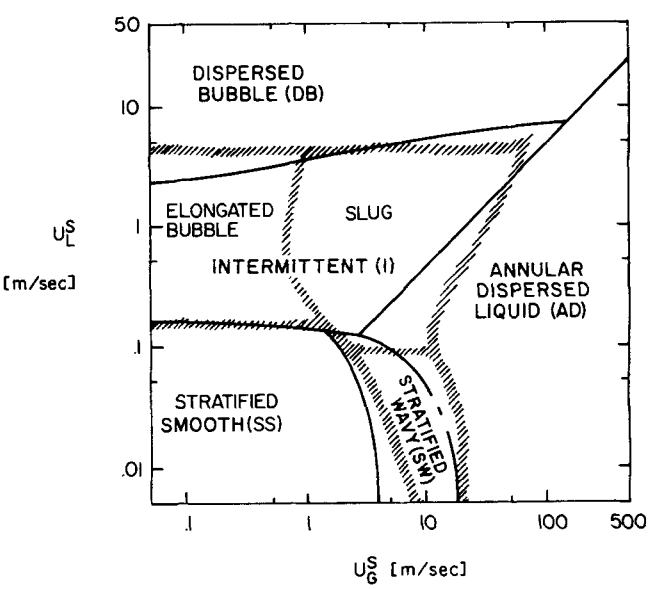

Fig. 2. A comparison of experiment with theoretically predicted flow regimes in horizontal tubes.

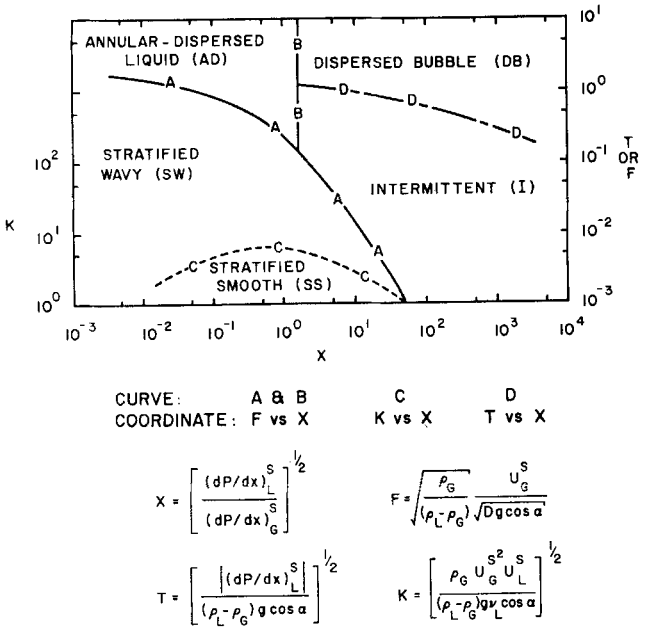

$$X = \left[\frac{(dP/dx)_L^S}{(dP/dx)_G^S}\right]^{1/2} \qquad F = \frac{\rho_G}{\sqrt{(\rho_L-\rho_G)}}\frac{U_G^S}{\sqrt{Dg\cos\alpha}}$$

$$T = \left[\frac{|(dP/dx)_L^S|}{(\rho_L-\rho_G)g\cos\alpha}\right]^{1/2} \qquad K = \left[\frac{\rho_G U_G^{S^2} U_L^S}{(\rho_L-\rho_G)gv_L\cos\alpha}\right]^{1/2}$$

Fig. 3. Generalized flow regime map for horizontal two phase flow.

In general, one can distinguish between two types of maps:

1. One based on physical coordinates as shown in Figure 2, where the superficial velocities of liquid and gas are used as coordinates.

2. One based on dimensionless groups. In this case the map will be general provided the correct dimensionless coordinates are chosen and if the physical processes involved in the transition depend on only two dimensionless groups.

In most existing maps, the transition lines in either physical or dimensionless coordinates are located by the use of experimental data. As a result, the maps are limited to the range of conditions of the data. Even where the coordinates are dimensionless groups, the generality of most existing maps is questionable, since in the past the choice of particular dimensionless coordinates has been based primarily on speculation.

In a recent paper, Taitel and Dukler (1976) proposed a generalized map which is based on physical modeling of the transition mechanisms and for which the transition lines are obtained by a mathematically predictive method for which no data are needed. The results yields a generalized map where two dimensionless coordinates are used for each transition. Because the mechanism for transition is different between each pair of flow patterns, the same pair of dimensionless coordinates is not common to each transition. However, the dimensionless group X is common to all transitions. Thus, a map could be constructed on a single diagram as shown in Figure 3. Note that slug flow and elongated bubble flow are considered the same flow pattern and designated intermittent flow as suggested by Hubbard and Dukler (1966). For given pipe size and fluid properties, the theory predicts that the transition boundaries depend only on the superficial velocities u_L^s and u_G^s. The solid curves of Figure 2 show the theoretically predicted transition boundaries for air/water in a 2.5 cm pipe at low pressure in comparison with the boundaries recommended by Mandhane which were based on experimental data for the same system. As shown, the agreement is good. For other pipe sizes and/or fluid properties, these boundaries change location in the $u_G^s - u_L^s$ plane.

The studies described above have been limited to steady state or equilibrium flow conditions, namely, the situation where liquid and gas rates are constant. If these rates are varied very slowly, transitions between flow patterns will take place at the same flow rates predicted for equilibrium conditions (Figure 2 or 3). In many engineering systems (and in particular in the case of breaks in pressurized water nuclear reactor piping), rapid changes in flow rate can be expected. It is important to predict the sequence of flow patterns which will be observed during these flow transients. If, for example, stratified smooth flow exists and the gas flow rate is increased slowly at constant liquid rate, a quasi equilibrium process will take place, and, as shown in Figure 2, the pattern will change from smooth stratified to wavy stratified flow and then to annular flow at the gas flow rates given in Figure 2. As will be shown, the system behaves differently for an abrupt change in flow rates. For example, when one increases gas flow rate, the change from stratified smooth to stratified wavy and to annular can occur at different gas rates than what would have been predicted for equilibrium or steady state conditions. Furthermore, it is possible by rapidly increasing gas flow rate to go through a temporary slug flow pattern before reaching annular flow. Thus, the path for unsteady flow pattern transitions may differ from that for quasi steady state flow.

Very little work has been done along these lines. French (1975) considered transient fluid flow regimes in a blowdown test simulating breakage of nuclear reactor piping. With his apparatus it was not possible to observe the flow regimes, and they were inferred through density measurements. Recently, Sakoguchi et al. (1973) reported observations on the transient behavior when gas or liquid flow rate is increased. He showed that the transient path may differ from its quasi steady state path both in terms of the flow patterns observed and the flow rates at which transitions occur. No theoretical framework was presented for these results.

In this paper, the flow pattern behavior of two phase flow under transient conditions is analyzed theoretically and experimentally and a model proposed by which the expected regimes can be predicted.

THEORY

Mechanism for Steady State Equilibrium Transitions

As a basis of extending the theory for steady state transitions to the unsteady state case, it is useful to summarize the main ideas given in the earlier work (Taitel and Dukler, 1976). A solution for steady flow is developed by which the liquid level in the pipe is calculated for equilibrium stratified flow. If the conditions for equilibrium stratified flow are unstable, transition may occur as follows:

1. Transition between stratified and intermittent or annular pattern: this transition is visualized to take place as a result of Helmholtz instability causing waves of finite size on a stratified film. This instability is caused by the decrease of the pressure over a large wave due to the Bernoulli effect when gas accelerates over the wave crest. The transition to the intermittent or annular pattern occurs when the upward Bernoulli forces resulting from the decrease of the pressure over the wave overcomes the downward gravity forces.

2. Transition between intermittent and annular pattern: a transition to intermittent flow is visualized to occur when blockage of the gas passage by the growing wave forms a competent bridge causing a slug or plug to form. At high gas flow rate, the liquid level in the pipe is very low. In this case, even though an unstable wave of finite size is formed and tends to grow, there is not enough liquid to support building of a slug. In this case, the gas

drives the waves around the wall, and annular flow will result.

3. Transition between stratified smooth and stratified wavy pattern: this transition is related to the phenomenon of wave generation on a smooth gas-liquid interface. The mechanism is quite complicated and not yet completely understood. Nevertheless, it is generally accepted that waves form when pressure and shear work on the wave overcome the viscous dissipation in the wave. In this formulation, Jeffreys' approach is used which predicts the condition for wave initiation given knowledge of the sheltering coefficient. The value of this sheltering coefficient has been obtained both experimentally and theoretically.

4. Transition between intermittent and dispersed bubble: this transition is visualized as taking place when the liquid velocity is so high that turbulent fluctuations in the liquid which tend to dispense the gas overcome buoyancy forces acting on the gas bubbles.

Based on the models described above, the following equations were developed to predict the condition for transition.

Transition A: stratified to intermittent or annular

$$u_G \geq \left(1 - \frac{h}{D}\right) \left\{ \frac{(\rho_L - \rho_G) g A_G}{\rho_G A_L'} \right\}^{1/2} \tag{1}$$

Transition B: intermittent to annular

Equation (1) is satisfied and
$h/D < 0.5$ annular
$h/D \geq 0.5$ intermittent

Transition C: stratified smooth to stratified wavy

$$u_G \geq \left\{ \frac{400\, \nu_L (\rho_L - \rho_G) g}{\rho_G u_L} \right\}^{1/2} \tag{2}$$

Transition D: intermittent to dispersed bubble

$$u_L \geq \left\{ \frac{4A_G}{S_i} \frac{g}{f_L} \left(\frac{\rho_L - \rho_G}{\rho_L} \right) \right\}^{1/2} \tag{3}$$

The resulting theoretical transition lines expressed in generalized dimensionless coordinates appear in Figure 3. Note that once fluid properties and pipe size are set, all quantities in these equations depend only on the liquid level h and the two flow rates. Thus, this level plays the central rule, and its prediction is a necessary first step.

Transitions During Flow Transients

The approach to modeling flow pattern transitions under transient flow conditions parallels that for steady flow. First, the stable stratified liquid level is predicted, but in this case this level varies with position along the pipe x and time t. The stability of this level to the disturbances which underlie the transitions is explored as the flow transient proceeds according to the four criteria previously stated. As seen, these criteria all depend on liquid level. Under steady conditions, this level is invariant with time. Under transient conditions, the liquid level as well as the fluid velocities are time dependent. As will be shown, under conditions of transient flow and depending on the nature of the transient, flow pattern transition will take place at flow rates different from those expected for steady, equilibrium conditions. This happens because the liquid level during a transient is such that the transition can be satisfied at different rates than for equilibrium conditions. Furthermore, under certain conditions, in moving from one flow condition to another, flow regimes will appear that would not exist if the flow changes along this path were executed slowly.

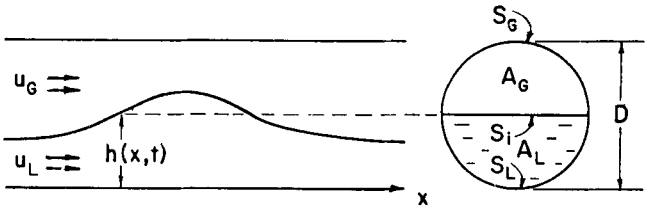

Fig. 4. Stratified flow geometry.

Equations for Liquid Level Under Transient Flow Conditions

Figure 4 shows the geometry of stratified flow. Liquid and gas enter the pipe at $x = 0$, both flowing in the positive x direction. Under transient flow conditions, the gas-liquid interface is, in general, not parallel to the x axis; thus the liquid level h, average liquid velocity u_L, and average gas velocity u_G are all functions of x and t. Likewise, the liquid and gas cross-sectional areas A_L and A_G and the contact perimeter between the liquid and wall S_L gas and wall S_G and liquid gas interface S_i are all functions of the local liquid level h and thereby also depend on time and position.

The momentum and continuity equations for the liquid phase are given by

$$\rho_L \frac{\partial (u_L A_L)}{\partial t} + \rho_L \frac{\partial (u_L^2 A_L)}{\partial x} = -\tau_L S_L + \tau_i S_i - A_L \rho_L g \frac{\partial h}{\partial x} - A_L \frac{\partial P}{\partial x} \tag{4}$$

$$\frac{\partial A_L}{\partial t} + \frac{\partial (u_L A_L)}{\partial x} = 0 \tag{5}$$

S_L and S_i are given by

$$S_L = 2r \left[\pi - \cos^{-1}\left(\frac{h}{r} - 1 \right) \right] \tag{6}$$

$$S_i = 2r \sqrt{1 - \left(\frac{h}{r} - 1 \right)^2} \tag{7}$$

Since the cross-sectional area of the liquid film depends on the level of the liquid in the pipe, $A_L = A_L(h)$. Thus, Equations (4) and (5) take the form

$$g \frac{\partial h}{\partial x} + \frac{\partial u_L}{\partial t} + u_L \frac{\partial u_L}{\partial x} = -\frac{\tau_L S_L}{\rho_L A_L} + \frac{\tau_i S_i}{\rho_L A_L} - \frac{1}{\rho_L} \frac{\partial P}{\partial x} \tag{8}$$

$$\frac{\partial h}{\partial t} + u_L \frac{\partial h}{\partial x} + \frac{A_L}{A_L'} \frac{\partial u_L}{\partial x} = 0 \tag{9}$$

For a rectangular pipe, $A_L = hb$; for circular pipes, the liquid cross-sectional area as a function of the elevation from the bottom of the pipe is given by

$$A_L = r^2 \left\{ \pi - \cos^{-1}\left(\frac{h}{r} - 1 \right) + \left(\frac{h}{r} - 1 \right) \sqrt{1 - \left(\frac{h}{r} - 1 \right)^2} \right\} \tag{10}$$

and its derivative is

$$A'_L = \frac{dA_L}{dh} = 2r \sqrt{1 - \left(\frac{h}{r} - 1 \right)^2} \tag{11}$$

For calculating τ_L and τ_i, the conventional relations are used with the additional condition that the gas velocity is

much larger than the liquid velocity and that the liquid interface may be assumed to be smooth. In this case

$$\tau_L = f_L \frac{\rho_L u_L^2}{2} \qquad \tau_i = f_G \frac{\rho_G u_G^2}{2} \tag{12}$$

For f_L and f_G, a Blasius type of correlation is convenient for both the liquid and the gas

$$f = C\, R_e^{-n} \tag{13}$$

where C and n are chosen according to the condition of flow (turbulent or laminar) that exist in the liquid or gas. In most cases, both fluids will be turbulent, for which $C = C_L = C_G = 0.046$ and $n = n_L = n_G = 0.2$. The Reynolds number is based on the hydraulic diameter. For this purpose, the liquid is treated as if it flows in an open channel and $D_L = 4A_L/S_L$, whereas the gas is visualized as flowing in a closed duct bounded by the wall and the interface and thus $D_G = 4A_G/(S_i + S_G)$.

Next consider the equation of motion for the gas phase. The pressure gradient in the liquid and the gas is assumed to be equal, and Equations (4) and (5) with suitable subscripts are equally valid for the flow of the gas. The gas velocity is much greater than that of the liquid, and since gas flow rate changes are propagated down the pipe very rapidly compared to the liquid, a quasi steady state is assumed with respect to any time interval in which changes in liquid flow or level are significant:

$$\rho_G \frac{\partial (u_G^2 A_G)}{\partial x} = -\tau_G S_G - \tau_i S_i - A_G \frac{\partial P}{\partial x} \tag{14}$$

$$A_G u_G \rho_G = W_G = \text{const} \tag{15}$$

Substitution of (14) and (15) into (8) yields

$$\left[g - \frac{\rho_G}{\rho_L} \left(\frac{W_G}{\rho_G A_G} \right)^2 \frac{A'_L}{A_G} \right] \frac{\partial h}{\partial x} + \frac{\partial u_L}{\partial t} + u_L \frac{\partial u_L}{\partial x} = -\frac{\tau_L S_L}{\rho_L A_L} + \frac{\tau_i S_i}{\rho_L} \left(\frac{1}{A_L} + \frac{1}{A_G} \right) + \frac{\tau_G}{\rho_L} \frac{S_G}{A_G} \tag{16}$$

$$\frac{\partial h}{\partial t} + u_L \frac{\partial h}{\partial x} + \frac{A_L}{A_L'} \frac{\partial u_L}{\partial x} = 0 \tag{17}$$

Equations (16) and (17) are two simultaneous partial differential equations for $h(x, t)$ and $u_L(x, t)$. Note that the right-hand side of (16) is a known function of h and u_L. Also note that for steady equilibrium conditions, namely, the case where the liquid level is constant, the left-hand side of (16) is identically zero, and Equation (16) becomes identical to Equation (6) in the paper by Taitel and Dukler (1976).

Approach to Solution of the Equations

Equations (16) and (17) predict the transient variation of the local liquid level and local average velocity as the flow condition is varied from one state to another. The knowledge of the instantaneous liquid level with the application of the mechanisms for transition as discussed above indicate when transition will occur.

Equations (16) and (17) are two hyperbolic, partial differential equations provided

$$g >> \frac{\rho_G}{\rho_L} \left(\frac{W_G}{\rho_G A_G} \right)^2 \frac{A'_L}{A_G} \tag{18}$$

Unless (18) is satisfied, a unique solution to these equations does not exist (Taitel and Dukler, 1977). Calculations show that even at flow rates closely approaching these for instability of the stratified flow, the Bernoulli term is, in fact, negligible compared to gravity. But neglecting this term can also be justified on a physical basis as well. Physically, the right-hand side of (18) describes the Bernoulli forces opposing gravity that act on the fluid when the gas is accelerated to high velocity over the crest of a wavy interface. In order to avoid this mathematical problem, the approach to the solution of (16) and (17) is to predict the variation of smooth liquid level profile and velocity with time in the absence of local waves. At each point in space and time, the local stability of the surface to wave growth due to Bernoulli forces is explored using the criteria of Equation (1). Consistent with this approach, the Bernoulli term is neglected in (16). While this approach provides a device to overcome mathematical difficulties, it is also consistent with the physical behavior as observed in flow of gas, and liquid level is stratified near the entry. Waves formed on this surface travel and grow as they move downstream as if superimposed on a smooth stratified surface.

Once the Bernoulli term in (16) is neglected, Equations (16) and (17) take the form

$$\frac{\partial u_L}{\partial t} + u_L \frac{\partial u_L}{\partial x} + g \frac{\partial h}{\partial x} + E = 0 \tag{19}$$

$$\frac{\partial h}{\partial t} + u_L \frac{\partial h}{\partial x} + H \frac{\partial u_L}{\partial x} = 0 \tag{20}$$

where $H = H(h) = A_L/A'_L$, and $E = E(h, u_L)$ is minus the right-hand side of Equation (16).

Using standard methods (Stoker, 1957), we can convert Equations (19) and (20) to

$$\left[(u_L + C) \frac{\partial}{\partial x} + \frac{\partial}{\partial t} \right] u_L + \sqrt{\frac{g}{H}} \left[(u_L + C) \frac{\partial}{\partial x} + \frac{\partial}{\partial t} \right] h + E = 0 \tag{21}$$

$$\left[(u_L - C) \frac{\partial}{\partial x} + \frac{\partial}{\partial t} \right] u_L - \sqrt{\frac{g}{H}} \left[(u_L - C) \frac{\partial}{\partial x} + \frac{\partial}{\partial t} \right] h + E = 0 \tag{22}$$

where $C = \sqrt{gH}$ is the critical velocity.

Equations (21) and (22) were solved using the finite-difference technique described by Stoker (1957). In this method, explicit forward finite differences are used with respect to time, whereas the spacial derivative is replaced by either forward or backward finite differences depending on the direction of the characteristic lines. Equation (21) is associated with the forwards characteristic which has a slope $dx/dt = 1/(u_L + C)$, and thus backward finite differences are used. Equation (22) is associated with the characteristics having the slope $dx/dt = 1/(u_L - C)$. When, at a given x and t, $u_L > C$, or the flow is supercritical, the direction of the characteristics associated with (22) is positive, and a backward finite spacial differentiation is used. At subcritical conditions when $u_L < C$, forward differentiation is used.

In the numerical scheme, each point is checked to determine whether the flow is sub or supercritical and the appropriate forward or backward numerical scheme selected. In order to insure stability, the time increment Δt is limited by $\Delta t < \Delta x/(u_L + C)$.

The boundary conditions needed for the solution of (21) and (22) depend on whether the local conditions is sub or supercritical. For the supercritical case $h(x, 0)$, $u_L(x, 0)$, $u_L(0, t)$, and $h(0, t)$ are required as boundary

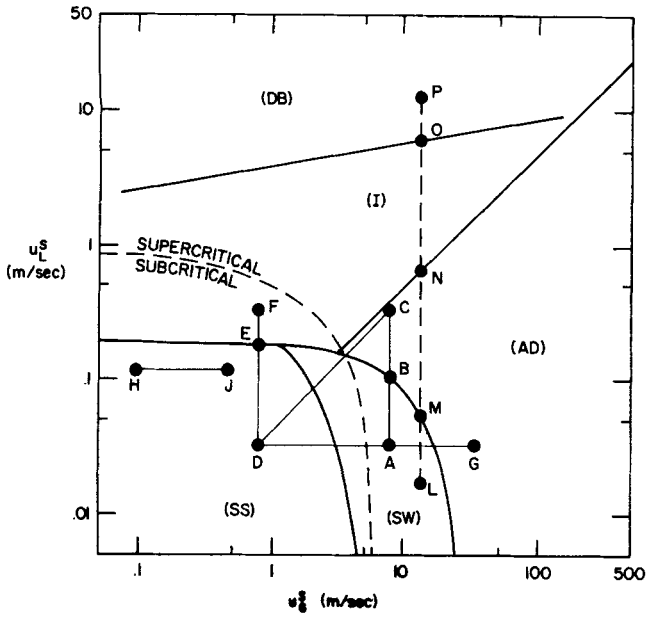

Fig. 5. Flow transients:air-water in 3.8 cm pipe at 25°C, 1 atm.

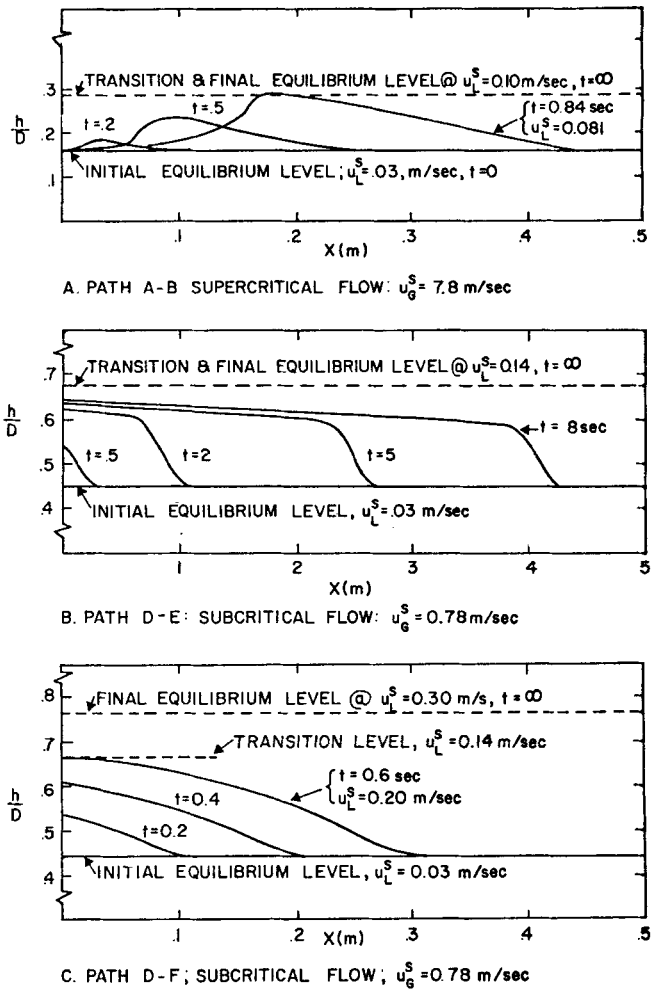

Fig. 6. Increasing liquid rate at constant gas rate:total flow transient time = 1.0 sec.

and initial conditions. When the flow is subcritical, only $h(0,t)$ or $u_L(0,t)$ can be assigned, since they are related through Equation (22) and are associated with the backward characteristics. In this case, however, the flow rate is specified, and for the subcritical case both $u_L(0,t)$ and $h(0,t)$ are determined by the flow rate.

Note that $H = A_L/A'_L$ and $C = \sqrt{gH}$. As seen from Equations (10) and (11), H depends uniquely on h/r, and for any set of fluid properties, this depends uniquely on $u_L{}^S$ and $u_G{}^S$ as shown by Taitel and Dukler (1976). The locus of points in the $u_L{}^S - u_G{}^S$ plane under equilibrium conditions along which $u_L = C$ is shown as a dotted curve in Figure 5 for the low pressure air-water system.

A variety of solutions can be generated by this analysis. Three basic processes are discussed: changing liquid rate at constant gas rate, changing gas rate at constant liquid rate, and simultaneous change in gas and liquid rate.

Changing Liquid Rate

As a first example, consider the flow of water and air at 25°C, 1 atm, in a 3.8 cm diameter pipe where the steady initial flow rates correspond to $u_L{}^S = 0.03$ m/s designated as point A in Figure 5. Stratified wavy flow exists under this condition. The liquid flow rate is increased to $u_L{}^S = 0.1$ m/s at B as shown in Figure 5. Point B is on the transition line from wavy stratified to annular flow under equilibrium conditions. If this process is carried out very slowly, the system passes through a series of equilibrium states during which the liquid level (which is constant for all x positions) increases, and, correspondingly, the true gas velocity increases. As outlined by Taitel and Dukler (1976), precisely at B the surface becomes unstable to finite wavy disturbances because Equation (1) is satisfied. If the h/D when this condition is satisfied exceeds 0.5, then intermittent flow is observed. When it is below 0.5, the flow pattern becomes annular.

Now consider this same change in liquid flow rate from A to B taking place rapidly. In Figure 6*a*, the change of the liquid level with time is plotted as the liquid rate is linearly increased from point A to B (Figure 5) in 1.05 Note that for this case the flow is supercritical at all points and all times. Consistent with the requirement of supercritical flow, the level at the entry remains constant. The fast moving liquid is shown to accumulate near the entrance region when the liquid rate is increased to create a local hump. When any position of this hump reaches the transition level [that is, Equation (1) is satisfied], the gas velocity over the hump causes instability of the liquid surface to waves, and local transition to annular or slug flow takes place.

In this example the transition level is reached in 0.84 s at a liquid flow rate of 0.091 m/s, 9% below the flow rate that would cause transition if the change were made very slowly. Thus, the analysis predicts somewhat earlier transition in this case.

Path D-E represents an increase of liquid flow rate under subcritical conditions. The solution for liquid level change is seen in Figure 6*b*. As can be observed, the subcritical case behaves totally different from the supercritical one. Under these conditions, the liquid accumulates at the entrance as a result of a rising level there. The slope of the liquid surface at the advancing front steepens and propagates downstream as a bore. At $x = 0$, the level asymptotically approaches the equilibrium level of E. Following the criterion for transition, Equation (1), slugging conditions are reached when the entry region level reaches the transition conditions of point E. The solution indicates that this will happen only asymptotically with time and well beyond the time when the final flow rate is reached. When the liquid is linearly increased from D to F in 1.0 s, the solution given in Figure 6*c* shows that at $x = 0$ the level reaches the transition conditions only after the liquid flow rate corresponding to E has been passed. Thus, in this instance, transition to slugging is delayed and occurs at $u_L{}^S =$

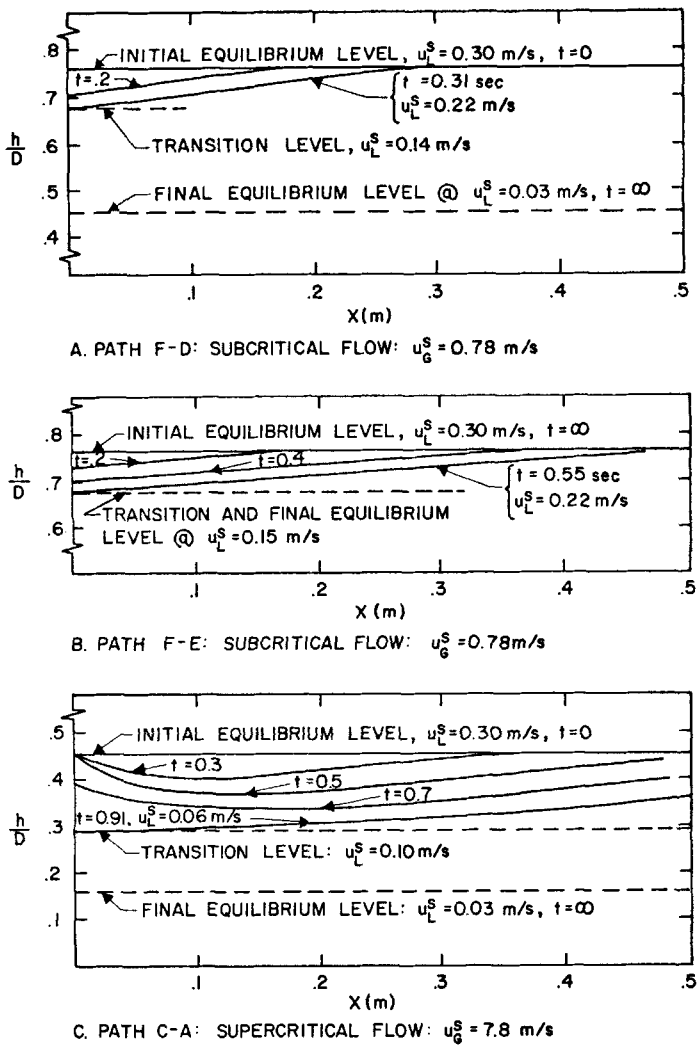

Fig. 7. Decreasing liquid rate at constant gas rate:total flow transient time = 1.0 sec.

0.20 m/s instead of at the steady state transition value of $u_L^S = 0.14$ m/s. Note the important difference in the effect of rapidly increasing liquid flow rate when the path is totally above or totally below critical flow velocities. Above the critical state for increasing liquid rate, the onset of transition is advanced, taking place at liquid rates below those which would cause transition under equilibrium conditions. For subcritical flow, the transition is delayed and takes place at flow rates higher than would be experienced under a very slow change in liquid rate.

Level variations with time and position for cases of decreasing liquid flow rate are shown in Figure 7. The paths considered are the reverse of those discussed above (F to D where the liquid rate is decreased while being in the subcritical region, path F-E where E is located on the transition line, and finally the path C-A which is in the supercritical region). The solutions show that as the liquid flow rate is decreased rapidly, the liquid level drops near the entrance. For the subcritical cases, the level is at its lowest at $x = 0$, whereas for the supercritical case, the level reaches a minimum at $x > 0$. During the first 0.5 s of the transient along the path 6-A (Figure 7*c*), the flow is supercritical. After this initial period, the flow becomes subcritical near the entrance as indicated by the shift in the minimum to the location $x = 0$.

Under transient conditions, the transition is assumed to take place at the first instant in time that the liquid level at any x reaches the transition level, that is, when Equation (1) is an equality. For example, for path F-D of Figure 5, changing flow rate very slowly would result in the transition from intermittent to smooth stratified flow at $u_L^S = 0.14$ m/s. However, if the change from F to D is made in 1 s, the liquid level (Figure 7*a*) drops to the transition value at $x = 0$ after only 0.31 s at which point the liquid rate has dropped to only $u_L^S = 0.22$ m/s. Even though the level at $x > 0$ exceeds the transition level, slugging is expected to stop when $h(x = 0)$ falls to the transition level because slug formation ceases at $x = 0$ and the last slug formed prior to $t = 0.31$ s is rapidly swept out of the tube. After this last slug passes, the liquid level in the tube is the height of the residual film left by the slug.

Executing the change F-E in 1.0 s results in the transition taking place after 0.55 s at a liquid rate $u_L^S = 0.23$ m/s. In fact, beyond 0.55 s the level at $x = 0$ will drop below the level of the final equilibrium state.

When the liquid rate is decreased along the path C-A, the initial state being supercritical, the result is different from the above in that there is a delay in the transition, as seen from Figure 7*c*, where liquid level profiles are shown during a linear change from C to A programmed for 1.0 s. The transition level is reached after 0.91 s and at $u_L^S = 0.06$ m/s. If equilibrium conditions were to exist during this change, the transition would take place at 0.74 s and a flow rate of $u_L^S = 0.10$ m/s.

The above examples demonstrate that opposite trends are observed when the initial conditions are in the sub and supercritical flow states. As liquid rate is increased, transition is reached earlier than expected for supercritical flow and is delayed for subcritical flow. The opposite effects take place for rapid decreases in liquid flow rate.

It is important to emphasize that the mechanism for transition under transient flow conditions is identical to that for steady flow conditions. For the six paths shown in Figures 6 and 7, this takes place when, as the flow rate of liquid is changed, Equation (1) is first satisfied at some location x. However, the flow rates at which this condition is satisfied differs from those for equilibrium conditions shown on the map of Figure 5.

All of the above paths were selected to display only one transition. However, unsteady state paths across several transitions, such as L, M, N, O in Figure 5, can be calculated in the same manner with the applicable criteria discussed above.

Changing Gas Rate

Equations (19) and (20) have been solved numerically for liquid level profiles as the gas rate is changed with liquid rate held constant. The paths are A-G and D-G in Figure 5. The profiles for increasing and decreasing gas flow rates appear in Figures 8 and 10. Shown in each case are the time and gas flow rates at which transition will take place. Characteristic of all these cases, the liquid levels and velocities are very slow to respond to changes in gas rate. In most cases, at some value of x the level has changed negligibly in the time interval that the gas rate has changed sufficiently to cause transition. This is to be expected, since the gas influences the liquid through interfacial shear, and this requires a relaxation of the initial velocity distribution in the liquid.

Consider path A-G and the liquid profiles shown in Figure 8*a*. At the initial conditions of $u_G^S = 7.8$ m/s and $u_L^S = 0.03$ m/s, the flow is wavy stratified. The gas flow is programmed to increase to 30.5 m/s. Transition to annular flow takes place at $t = 0.24$ s, at which point u_G^S has increased to 13.1 m/s. At this instant the flows and levels are such as to satisfy Equation (1). Since h/D

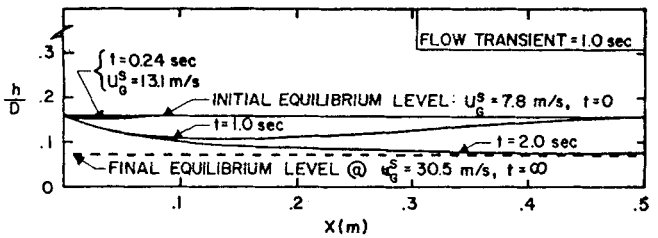

A. PATH A-G: SUPERCRITICAL FLOW: u_L^S = 0.03 m/s
TRANSITION AT t = 0.24 sec

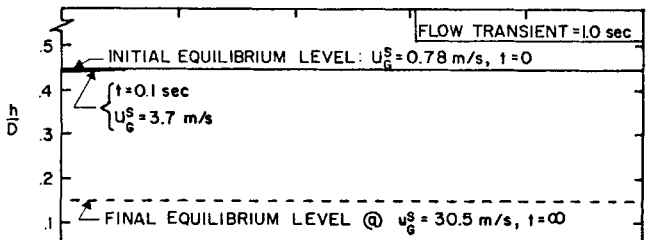

B. PATH D-G: INITIALLY SUBCRITICAL FLOW: u_L^S = 0.03 m/s
TRANSITION AT t = 0.1 sec

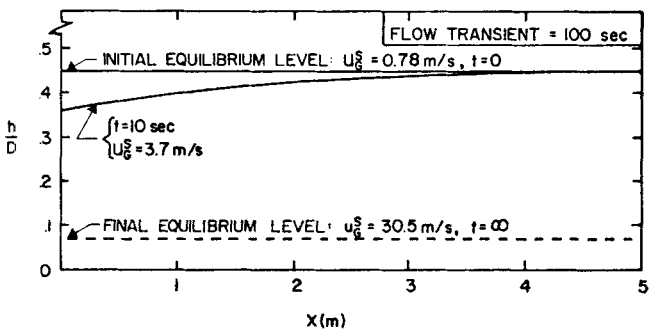

C. PATH D-G: INITIALLY SUBCRITICAL FLOW: u_L^S = 0.03 m/s
TRANSITION AT t = 10 sec

Fig. 8. Increasing gas rate at constant liquid rate.

< 0.5, the transition takes place to annular flow. The mechanism for this early transition can be seen from Figure 9, which shows the variation in h/D, u_G, and ϕ as the gas flow rate (expressed as $u_G{}^S$) is increased. An unstable interface will exist and transition will take place when, according to Equation (1), $u_G \geq \phi$. The solid lines represent the result when the change takes place through a series of quasi equilibrium states. It is seen that transition will take place when $u_G{}^S$ reaches 16.5 m/s.

Now consider the results if the transient takes place in 1.0 s. The liquid level has insufficient time to respond to the transient in the gas as shown in Figure 8*a*. In fact, after 1.0 s the liquid level downstream is essentially unchanged from its original value. Both the gas velocity and ϕ are at a maximum where the level is highest. The maximum values of h/D, u_G, and ϕ are plotted as dotted lines in Figure 9. The condition $u_G \geq \phi$ is met at gas rate of 13.1 m/s, lower than would take place under equilibrium conditions.

Consider path D-G in Figure 5 with a linear change in gas rate from 0.78 to 30.5 m/s taking place in 1.0 s. The flow pattern of the initial state is smooth stratified.

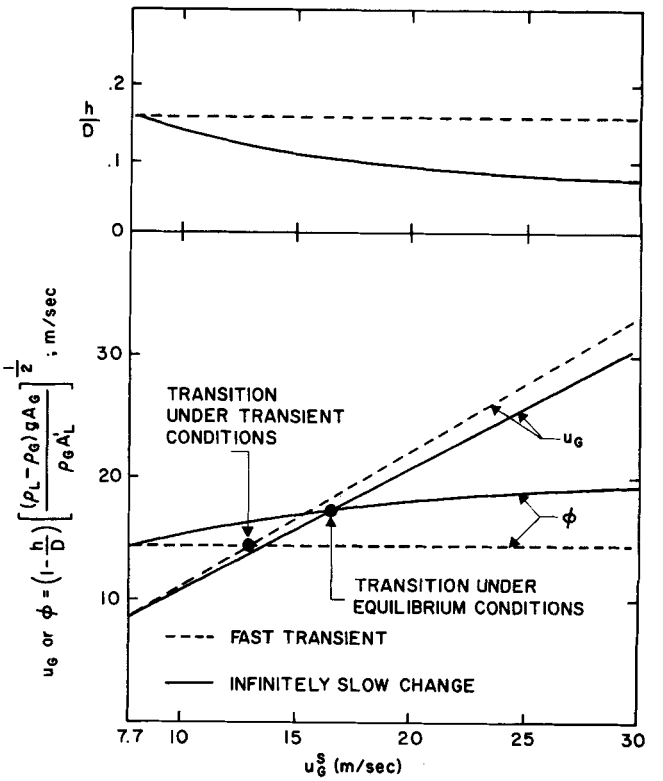

Fig. 9. Satisfying the instability criteria for fast gas transients vs. equilibrium change.

The liquid profile after 0.10 s is shown in Figure 8*b*. Again, it is evident that the liquid level is essentially unchanged. In the early stages of the transient, Equation (2) is satisfied after 0.043 s when the gas rate $u_G{}^S$ reaches 2.0 m/s and transition to wavy stratified flow takes place. Under equilibrium conditions, this would take place at $u_G{}^S = 3.4$ m/s. As the transient proceeds, Equation (1) is satisfied after 0.1 s when $u_G{}^S$ reaches 3.7 m/s. Since at that instant $h/D > 0.5$, transition to annular flow takes place. This compares with $u_G{}^S = 16.5$ m/s at which steady state transition would take place.

Less rapid gas transients can result in the liquid level changing significantly at least in the entry region before the end of the transient period. Traversing path D-G in 100 s results in the liquid profiles shown in Figure 8*c* for $t = 0$ and $t = 10$ s. However, even after 10 s and for $x \geq 4$ m the level is essentially unchanged. Transitions A, B, and C take place at the location where the gas velocity is highest, and this occurs at the location of the highest liquid level. Thus, in general, these transitions will first be observed downstream when a transient involving increased gas rate is executed.

During a transient decrease in gas flow rate for fast and moderate transients, the change in liquid level is negligible up to the point in time that the gas flow rate changes enough to cause transition to take place. Figure 10 demonstrates this. Shown in each case is the profile at the instant at which the gas velocity is such that transition A from annular to stratified wavy flow [Equation (1)] takes place. At equilibrium, the transition would occur at $u_G{}^S = 16.5$ m/s. Under transient conditions, this takes place at higher velocities as follows:

Path	Transient time	Time to transition	$u_G{}^S$ at transition
G-A	1.0 s	0.53 s	18.0 m/s
G-D	1.0 s	0.40 s	18.6
G-D	100 s	30.0 s	21.0

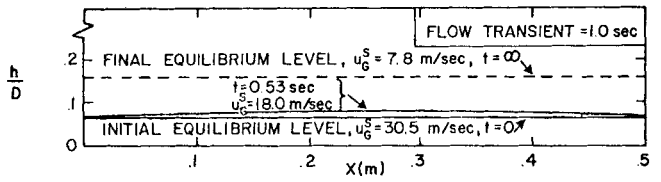

A. PATH G-A: SUPERCRITICAL FLOW: u_L^S=0.03 m/sec

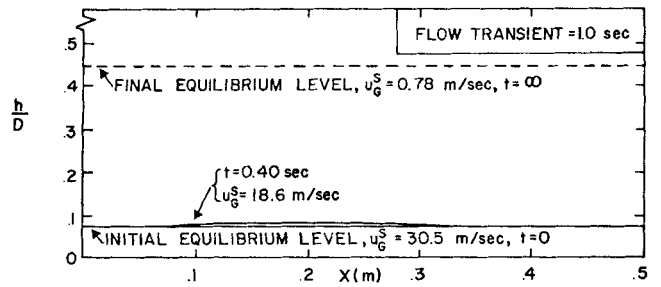

B. PATH G-D: INITIAL SUPERCRITICAL FLOW: u_L^S=0.03 m/sec

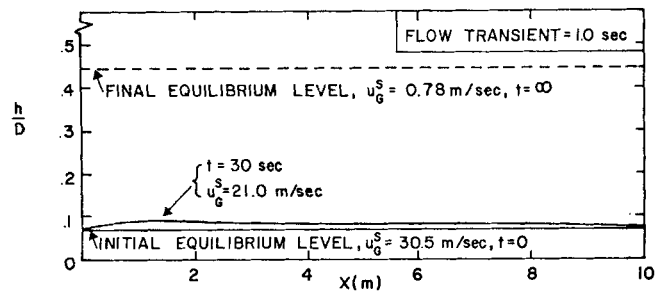

C. PATH G-D INITIAL SUPERCRITICAL FLOW: u_L^S=0.03 m/sec

Fig. 10. Decreasing gas rate at constant liquid rate.

The Appearance of Spurious Flow Patterns for Fast Transients

Define a fast transient as one where the liquid level remains essentially unchanged over the period of time it takes the gas rate to increase enough to result in transition. For these fast transients in gas flow rate, a particularly simple and elegant graphical procedure is available to predict the flow regimes encountered along the path and when the transitions can be expected to occur.

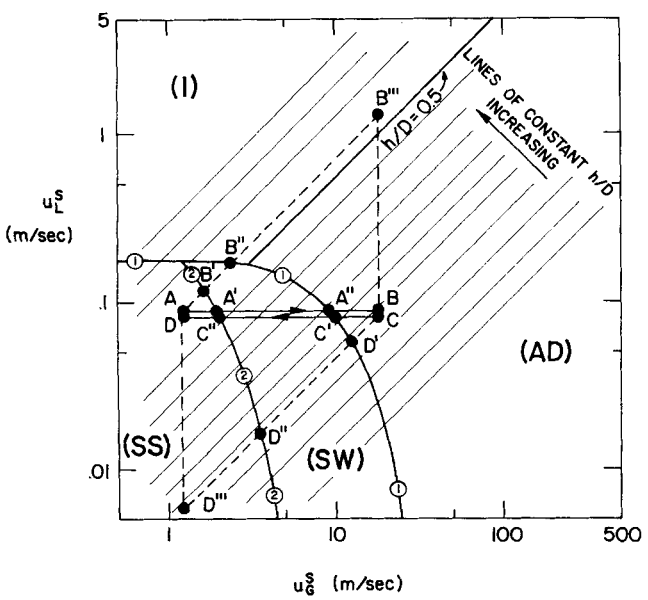

Fig. 11. Gas flow transients.

Transient changes in liquid flow rate at constant gas flow (paths D-F and A-C of Figure 5) display the same flow patterns as would be observed if the flow were changed in an equilibrium manner, but the transitions take place at different liquid flow rates. However, during a gas flow transient patterns not observed along the equilibrium path can appear. For example, consider the path H-J of Figure 5. The flow pattern in both the initial and final states is smooth stratified. Now execute a fast transient. The liquid level remains at its initial value as the gas rate increases. Testing Equation (1) along the path shows that u_G exceeds ϕ as soon as u_G^S is greater than 0.15 m/s. At this point, slugging will take place. Eventually, after the gas rate change is completed, the liquid level will drop to its equilibrium value, the gas velocity will decrease, and the system will return to smooth stratified flow.

All flow regimes which appear during a fast gas transient can be predicted by a simple graphical procedure using the equilibrium map. Furthermore, the time and the gas flow rate of which each transition will take place can be calculated. The method can be understood by reference to Figure 11. Consider the path A to B, where the gas rate is increased. If the process is carried out very slowly, the system will pass through a series of quasi equilibrium states along A-B, and transitions will be observed at each flow rate where the line A-B crosses a transition curve. Superimposed on this curve are a series of lines of constant equilibrium h/D. That such lines are straight with a slope of 45° on log-log coordinates follows from Taitel and Dukler's (1976) Figure 2 and Equation (8) for the case when both gas and liquid are in turbulent flow. A fast gas transient is one which, for at least some x location in the pipe, the initial level remains unchanged until the gas rate has reached its final value. Thus, the level remains constant at its initial value along the line A B′ B″ B‴ as the gas rate changes. But the intersection of this constant level line with the transition curves indicates precisely the gas flow rates which satisfy each transition criteria. Consider the transition to intermittent flow represented by the curve ① — ① in Figure 11 for equilibrium conditions. The right-hand side of Equation (1) depends only on h/D (aside from physical properties). Likewise, the left-hand side depends only on u_G^S and h/D; that is

$$u_G = \frac{u_G^S}{A_G/A}; \qquad \frac{A_G}{A} = \frac{A_G}{A}(h/D)$$

Thus, curve ① — ① can be considered the locus of points where h/D and u_G^S satisfy the equality in Equation (1), and the intersection of constant h/D lines with this curve indicates u_G^S at which this transition will take place. So it is seen that as the fast transient proceeds along the constant h/D path of A B′ B″ B‴, the stratified flow would change to slug flow at $(u_G^S)_{B''}$ and remain in slug flow until the gas flow rate has reached its final value. Then, as the level recedes with subsequent time to a value below 0.5, the pattern would change to annular along B‴-B.

A similar, although not as exact method, provides the condition for transition from smooth to wavy stratified flow during the fast gas transient. Curve ② — ② shows the conditions for this transition for equilibrium flows. As indicated, the left-hand side of the equation depends only on u_G^S and h/D. The right-hand side depends also on the liquid velocity u_L. However, during fast gas transient the liquid level is essentially unchanged, and the liquid flow rate is constant. Thus, u_L remains nearly constant, and the intersection of constant h/D lines with curve ② — ②

indicate the value of u_G^S at which this transition to wavy flow will take place. For the transient shown, this will occur at $(u_G^S)_{B'}$.

For transients with linear changes in gas flow rate, the time interval from the start to the appearance of stratified wavy and slug flow can be easily calculated. Designate τ as the time for the gas flow rate transient to be completed, τ_1 the time from $t = 0$ before wavy stratified flow appears, and τ_2 the time from $t = 0$ before the slug flow appears. Then

$$\tau_1 = \frac{(u_G^S)_{B'} - (u_G^S)_A}{(u_G^S)_B - (u_G^S)_A}\tau$$

$$\tau_2 = \frac{(u_G^S)_{B''} - (u_G^S)_A}{(u_G^S)_B - (u_G^S)_A}\tau$$

If the u_G^S does not change linearly with time, then the values of τ_i can be obtained from

$$(u_G^S)_{B'} - (u_G^S)_A = \int_0^{\tau_1} \frac{du_G^S}{dt}\,dt$$

$$(u_G^S)_{B''} - (u_G^S)_A = \int_0^{\tau_2} \frac{du_G^S}{dt}\,dt$$

Note that the transient path differs from the equilibrium one in that:

1. Intermittent (slug) flow appears.
2. The transition to wavy stratified flow takes place at a lower value of u_G^S than for the equilibrium path

$$(u_G^S)_{B'} < (u_G^S)_{A'}$$

3. The transition from stratified wavy flow to unstable intermittent or annular flow occurs at a lower gas rate

$$(u_G^S)_{B''} < (u_G^S)_{A''}$$

Executing a fast transient in the reverse direction C to D will produce different results as seen in Figure 11. Here, the path will effectively follow CD'D"D'"D rather than CC'C"D. The same flow patterns will be observed during the transient as during an equilibrium path. However, transitions will take place at higher gas rates: $(u_G^S)_{D'} > (u_G^S)_{C'}$; $(u_G^S)_{D''} > (u_G^S)_{C''}$.

This method provides a visual display of the true path to be expected during a fast transient, determines when unexpected flow patterns will appear during the transient, provides the values of the gas rates at which each transition will appear, and makes possible the calculations of the time at which each transition will take place. It is of interest that the speed of the transient has no effect on the path or the flow patterns which are observed.

Sakaguchi et al. (1973) also considered the problem of flow regime transitions during transient flow conditions. They made observations of the patterns which appeared during the transient and plotted the results as families of lines on a steady state map. However, the results are not general, and no theoretical basis was given.

For purposes of illustration, additional fast gas transient examples are mapped in Figure 12:

1. Process J-K, when executed slowly, will show no change in flow pattern, being entirely within the wavy stratified regime. However, a fast transient will result in the temporary appearance of slug and annular flow in the course of the transient.

2. In moving from E to F under equilibrium conditions, only the transition from annular to stratified wavy flow will be observed. A fast transient will result in the path EF'F, and the stratified smooth pattern will be displayed before the final pattern of wavy stratified flow appears.

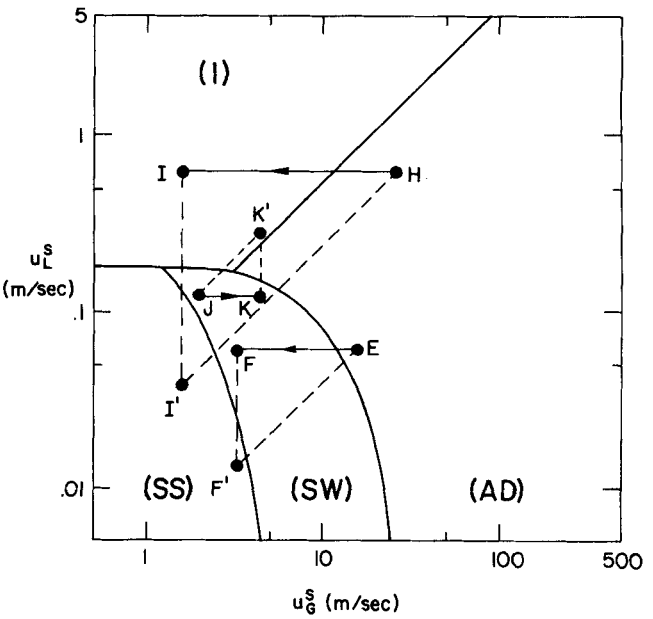

Fig. 12. Gas flow transient.

3. Of special interest is the path HI. For slow changes in gas flow rate, the conditions change from one highly agitated state to another (annular to intermittent). However, for a rapid gas transient, the model predicts a very quiescent period in the form of wavy stratified then smooth stratified flow before the system begins slugging again.

Simultaneous Transient Changes in Gas and Liquid Rates

Consider the path D-O in Figure 5, where both the gas and liquid flow rate are changed. In this case, the liquid level in the initial and final state are the same. If the process were carried out in an equilibrium manner, this level would remain constant for all x and t. The response of the liquid level for a 1.0 s linear transient of increasing flows appears in Figure 13*a*. The observed profiles represent the results of opposite effects. Increasing liquid rate tends to raise the level, while increasing gas rate suppresses the level. However, the effects are not equal, each varying in relative magnitude as the transient proceeds. The initial state D is at subcritical flow condi-

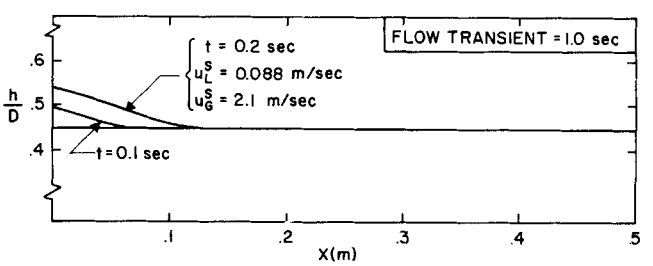

A. PATH D-C: LIQUID AND GAS RATE INCREASING

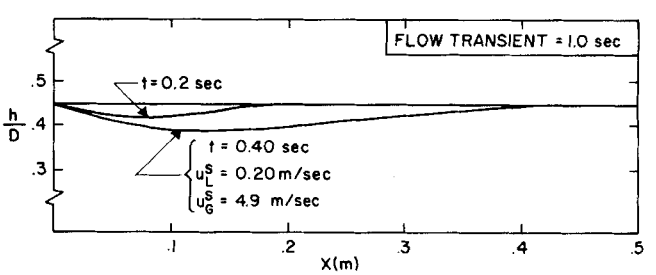

B. PATH C-D: LIQUID AND GAS RATE DECREASING

Fig. 13. Simultaneous change in gas liquid flow rates.

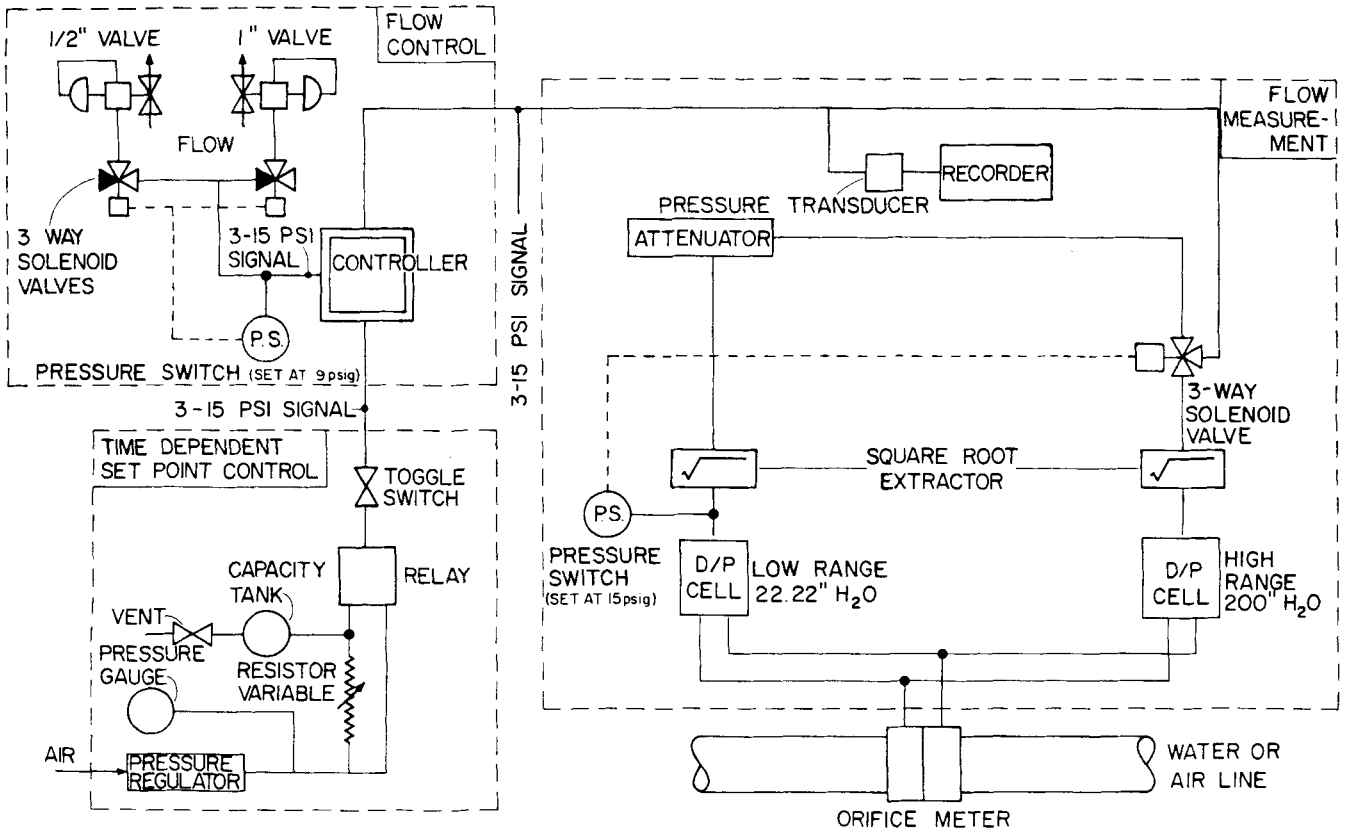

Fig. 14. Schematic arrangement of control system.

tions, and, as discussed previously, level changes are observed first at $x = 0$.

As the transient proceeds, the transition criteria Equations (1) and (2) are applied. The flow rates at which the transitions take place during the transient and equilibrium paths are compared below:

	u_G^S	u_L^S
Transition A:		
Transient	2.3 m/s	0.088 m/s
Equilibrium	3.9 m/s	0.14 m/s
Transition C:		
Transient	2.1 m/s	0.08 m/s
Equilibrium	2.0 m/s	0.06 m/s

Under equilibrium conditions, h/D is always less than 0.5, and thus transition A results in the formation of an annular flow. Figure 13*a* shows that at $t = 0.2$ s into the transient, when the gas velocity reaches 2.3 m/s and transition A takes place, $h/D > 0.5$ and a slug is formed at $x = 0$. Thus, the equilibrium path displays a sequence of flow patterns from smooth stratified to wavy stratified to annular. The transient path results in smooth stratified, changing to wavy stratified, followed by slugging, and then annular flow.

The situation for the reverse path C to D appears in Figure 13*b*. Since the initial condition is supercritical, the level at $x = 0$ remains constant, and a minimum appears at $x > 0$. The calculation was stopped at $t = 0.39$ s, where transition A takes place. Again, it is seen that this occurs at liquid and gas rates higher than for the equilibrium path.

The mechanisms presented above which explain transition during flow transients represent an idealization of a very complex process. In order to determine the validity of the proposed mechanisms for actual processes, experiments are necessary. To this end, an existing air-water loop with a long horizontal test section was instrumented to make possible transients in gas and liquid flow rates either independently or simultaneously and of varying time duration. The test section was transparent and permitted visual observation of the flow pattern.

EXPERIMENTAL EQUIPMENT

Flow Loop

The test pipe consisted of sections of 3.81 cm ID glass pipe joined together to form a length of 65 ft, as described by Dukler and Hubbard (1975). Water was recirculated in a closed loop and air supplied from an oil free, high capacity, rotary compressor. The air was vented from a separator located at the discharge of the test section. The entrance section consisted of a pipe divided by a plane at the center line to form two parallel flow channels, each consisting of a half cylinder.

Control System

Identical pneumatic control systems were installed for each phase. The schematic diagram for each is shown in Figure 14. Flow measurement was accomplished using differential pressure cells mounted on orifice meters. Two cells were required for each orifice in order to span the wide range of flow rates required. Pressure switches and a three-way valve as shown were used to make automatic switch over between d/p cells as the range of the low capacity cell was exceeded. The square root of the output pressure of the d/p cells which is directly proportional to flow rate was transmitted to a controller equipped with proportional and reset systems.

Flow control required two valves of different sizes in parallel on each stream in order to cover the required range of flow rates. A pressure switch and three-way valve system on the pneumatic signal provided automatic switch over as shown.

The transient in the flow was generated using a remote set point control system. The set point was changed over the full range of flows in response to a pneumatic signal. This signal could be varied with time by the use of a pneumatic analogue of a series RC circuit as shown in Figure 14. Capacitance was provided in the form of a small pressure tank. The resistance was a flow restriction whose coefficient of resistance could be varied.

TABLE 1. COMPARISON OF EXPERIMENT WITH THEORY: TRANSITION TO SLUGGING FOR AN INCREASING LIQUID FLOW TRANSIENT WITH INITIAL CONDITION SUBCRITICAL

	Gas	Liquid		Total transient	Time for 1st slug	Liquid rate at	Liquid flow rate at instability		Appearance of first slug	
		Initial	Final		to appear		Equilibrium	Transient	Rate	Time
	u_G^S	$(u_L^S)_1$	$(u_L^S)_2$	Δt	t_s	$t = t_s$ $(u_L^S)_s$	$(u_L^S)_e$	$(u_L^S)_i$	$(u_L^S)_s$	t_s
	Operating conditions				Experiment			Theory		
1.	0.77	0.077	0.61	11.8	5.6	0.33	0.14	0.14	0.32	5.4
2.	1.21	0.077	0.61	11.8	5.8	0.34	0.15	0.15	0.32	5.4
3.	3.05	0.077	0.61	11.8	6.0	0.35	0.15	0.16	0.30	4.9
4.	0.77	0.048	0.61	12.0	6.4	0.35	0.14	0.16	0.34	6.2
5.	1.21	0.048	0.61	12.0	6.9	0.37	0.15	0.17	0.34	6.2
6.	3.05	0.048	0.61	12.0	6.8	0.37	0.15	0.17	0.31	5.6
	m/s	m/s	m/s	s	s	m/s	m/s	m/s	m/s	s

Details of this sequence flow control system appears in the Appendix.

COMPARISON OF EXPERIMENT AND THEORY

Gas Flow Rate Transients

Rapid changes in gas flow rate with liquid flow held constant were carried out for each of the five paths shown in Figures 11 and 12 and between the initial and final states shown there. In each case, the flow transient was of approximately 3 s duration. The flow patterns as visually observed during the transient in every case were precisely predicted by the theory.

Sequence of flow patterns

Path	Predicted	Observed
A-B	Smooth strat.-wavy strat. -slug-ann.	Smooth strat.-wavy strat. -slug-ann.
C-D	Ann.-wavy strat.-smooth strat.	Ann.-wavy strat.-smooth strat.
E-F	Ann.-wavy strat.-smooth strat.-wavy strat.	Ann.-wavy strat.-smooth strat.-wavy strat.
H-I	Ann.-wavy strat.-smooth strat.-slug	Ann.-wavy strat.-smooth strat.-slug
J-K	Wavy strat.-slug-wavy strat.	Wavy strat.-slug-wavy strat.

This exact agreement with prediction not only gives validity to the model for transient conditions but directly verifies the models for steady state flow regime transition published earlier and the speculations as to mechanisms which are imbedded in those transition models.

The predicted time for transition to intermittent flow and the flow rate at this point during fast gas transients were measured and compared with the theory. Agreement was within measuring accuracy.

Liquid Flow Rate Transients

The theoretical analysis of flow regime transition for liquid flow transients with gas flow held constant as developed in the theoretical treatment above predicts:

1. *At subcritical liquid velocities* and for increasing rates, the transitions to intermittent and annular flows are delayed (take place at higher rates than would be expected during an equilibrium change). For this condition, as the liquid flow is increased, the level at the entrance rises rapidly before the level downstream changes significantly.

2. *For supercritical liquid flow* and when the transient involves an increase in liquid rate, the liquid level first rises at some location $x > 0$ to form a local hump. Under these conditions, the transition is advanced (occurring at flow rates less than those expected for an equilibrium change).

A repeated series of experiments were executed following a path similar to DE of Figure 5, where, in this case, E was located slightly below the u_L^S for equilibrium transition. As predicted (see Figure 6*b*), the level first rises at the inlet, and the level change propagates downstream with time as a bore. The flow remained stratified at all times with no temporary slugging, just as predicted by the theory.

Table 1 shows the flow conditions for experiments carried out with the initial state at subcritical conditions. Each run represents the arithmetic average of six experiments, with the change in liquid rate approximately linear with time.

Listed under operating conditions are the initial and final liquid flow rates of the transient and the total transient time Δt. The time at which the first slug was observed t_s and the measured liquid flow rate at that time $(u_L^S)_s$ are tabulated under experiment.

For these experiments, each of which result in transition to intermittent flow, the comparison with theory must be undertaken cautiously. At the instant during the transient at which the liquid level and gas velocity are such as to satisfy an equality in Equation (1), instability occurs and slugging becomes possible. However, slugs do not appear at that instant, and an additional waiting time is required before the first slug is observed. This waiting time τ_s is of the order of the inverse slug frequency. But τ_s is a function of the liquid rate, and this rate continues to increase as the transient proceeds during the waiting period. Thus, τ_s itself changes. In order to calculate the time to the appearance of a slug and the flow rate which would be observed at that time in the transient, it is necessary to have information on the variation of slug frequency with flow rate. In Figure 15, inverse frequencies are shown as functions of liquid rate for the three gas rates used in the experiments. It is seen that the time between slugs is extremely large just at the transition flow rate but decreases rapidly as liquid flow is increased.

With this information it is possible to predict the time for the appearance of the first slug. The method is easily accomplished graphically as shown in Figure 16. The construction is for the conditions of run No. 1 of Table 1. The solid line shows the path of the liquid flow transient u_L^S vs. t. The theory shows that at $t_1 = 1.4$ s into the transient, when $u_L^S = (u_L^S)_i = 0.14$ m/s, the surface becomes unstable and the waiting time begins. (In

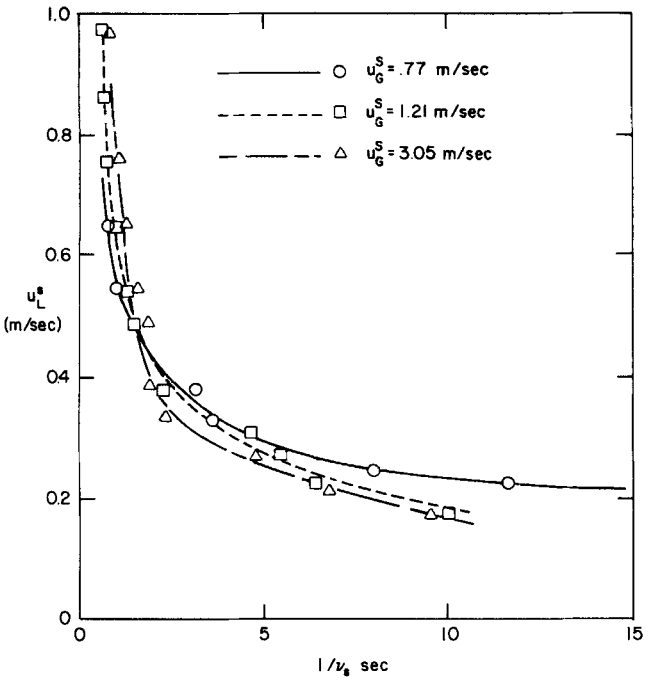

Fig. 15. Waiting time between slugs.

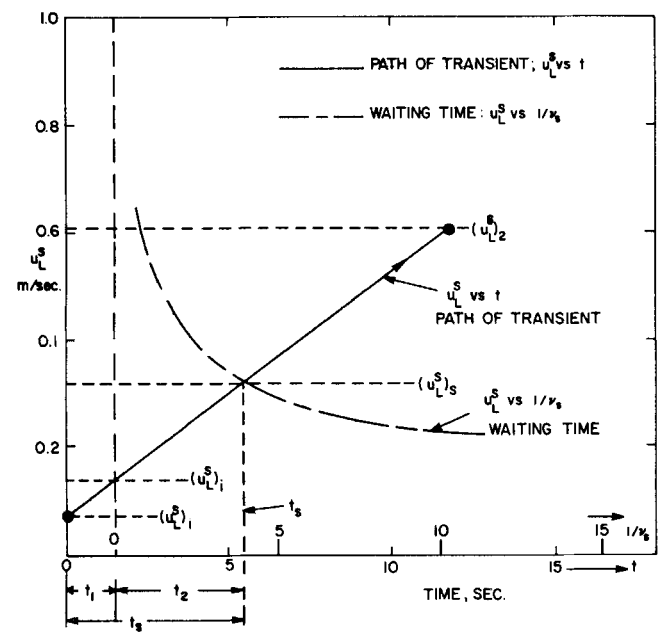

Fig. 16. Increasing liquid flow transient:determination of time to appearance of first slug for sub critical liquid velocity.

this particular instance, the flow rate at instability for the transient path is approximately equal to that for equilibrium change, but this is, in general, not the case.) As seen from the $1/\nu_s$ coordinate, as the transient proceeds, waiting time decreases. At the waiting time, $t_2 = 4.0$ s, the first slug is expected to form. The total time from the start of the transient is thus $t_1 + t_2$ or 5.4 s, and the value of $u_L{}^S$ at 5.4 s is 0.32 m/s. This compares with $u_L{}^S = 0.33$ m/s, at which the slug was observed to form. Table 1 shows that agreement between theoretically calculated and experimentally measured flow rates is good for all runs and well within the ability to discern the precise rate at the time the first slug forms. Similarly, the agreement between calculated and measured time is satisfactory.

The procedure for calculating the time and flow conditions for slugging to appear during a liquid flow transient which starts at subcritical conditions is as follows:

1. Calculate t_1 and $(u_L{}^S)_i$ from the theory for liquid level at the entry.
2. Calculate the waiting time from experimental data and/or theory on slugging frequency vs. flow rate (Taitel and Dukler, 1977) by finding the intersection between the path of the transient ($u_L{}^S$ vs. t) and the waiting time curve ($u_L{}^S$ vs. $1/\nu_s$). The initial condition for waiting time is $u_L{}^S = (u_L{}^S)_i$ at $t = 0$.
3. Sum $t_1 + t_2$ to find the time for appearance of the first slug. The flow rate at that time can be found from the path of the transient.

In many cases, t_1 is small compared to t_2, and in these cases the calculation is greatly simplified since the equilibrium value of $(u_L)^s$ can be used as an approximation for $(u_L{}^S)_i$.

Liquid flow transients were also executed, with initial conditions being above the critical liquid velocity and for increasing liquid rate with time. For these conditions, the flow rate change was so rapid and the flow pattern changes so gradual that precise quantitative data were impossible to obtain with the existing instrumentation. However, as predicted by theory, experiments showed that a local hump in the liquid level formed downstream of $x = 0$ immediately after initiation of the transient.

ACKNOWLEDGMENT

The financial support which made this work possible was provided by the U. S. Energy Research and Development Administration.

NOTATION

A = flow cross-section area
A'_L = differentiation with respect to h
b = width of rectangular pipe
C = friction factor constant [Equation (13)], also critical velocity $C = \sqrt{gH}$
D = pipe diameter, also hydraulic diameter
E = minus right-hand side of Equation (16)
f = friction factor
g = acceleration of gravity
h = liquid level
H = A_L/A'_L
n = exponent [Equation (13)]
P = pressure
r = pipe radius
R_e = Reynolds number
S = perimeter
t = time
t_s = time for first slug to appear
u = velocity in the x direction
W = mass flow rate
x = coordinate in the axial direction

Greek Letters

ν = kinematic viscosity
ν_s = slug frequency
ρ = density
τ = shear stress, time to complete transient
τ_s = waiting time between slugs

Subscripts and Superscripts

e = equilibrium
G = gas
i = gas-liquid interface
L = liquid
S = superficial, calculated as if the phase was flowing

along in the pipe
= differentiation with respect to h

LITERATURE CITED

Al-Sheikh, J. N., D. E. Saunders, and R. S. Brodkey, "Prediction of Flow Patterns in Horizontal Two-Phase Pipe Flow," *J. Chem. Eng.*, **48**, 21 (1970).

Alves, G. E., "Cocurrent Gas-Liquid Flow in a Pipeline Contactor," *Chem. Eng. Progr.*, **50**, 449 (1954).

Baker, O., "Simultaneous Flow of Oil and Gas," *Oil Gas J.*, **53**, 185 (July, 1954).

Bergelin, O. P., and C. Gazley, "Cocurrent Gas-Liquid Flow," *Heat Transfer* and *Fluid Mechanics Inst., Proc.* (May, 1949).

Dukler, A. E., and M. G. Hubbard, "A Model for Gas-Liquid Slug Flow in Horizontal and Near Horizontal Tubes," *Ind. Eng. Chem. Fundamentals* (1975).

French, R. T., "An Evaluation of Piping Heat Transfer, Piping Flow Regimes, and Steam Generator Heat Transfer for the Semiscale Model Isothermal Tests," *Aerojet Nuclear Co. Rept. ANCR 1229* (Aug., 1975).

Govier, G. W., and K. Aziz, *The Flow of Complex Mixtures in Pipes*, Van Nostrand Reinhold Co., New York (1972).

Govier, G. W., and M. M. Omer, "The Horizontal Pipeline Flow of Air-Water Mixtures," *Can. J. Chem. Eng.*, **40**, 93 (1962).

Hewitt, G. F., and N. S. Hall-Taylor, *Annular Two Phase Flow*, Pergamon Press, New York (1970).

Hoogendoorn, C. J., and A. A. Buitelaar, "The Effect of Gas Density and Gradual Vaporization on Gas-Liquid Flow in Horizontal Pipes," *Chem. Eng. Sci.*, **16**, 208 (1961).

Hubbard, M. G., and A. E. Dukler, "The Characterization of Flow Regimes for Horizontal Two-Phase Flow," *Proceedings of the 1966 Heat Transfer and Fluid Mechanics Institute*, M. A. Saad and J. A. Moller, ed., pp. 100-121, Stanford University Press, Calif. (1966).

Johnson, H. A., and A. H. Abou-Sabe, "Heat Transfer and Pressure Drop for Turbulent Flow of Air-Water Mixtures in a Horizontal Pipe," *Trans. ASME*, **74**, 977 (1952).

Kosterin, S. I., "Investigation of the Influence of Diameter and Inclination of a Tube on the Hydraulic Resistance of Gas-Liquid Mixtures," *Izvestiya Akademii Nauk., SSSR, O.T.N.*, **12**, 1824 (1949).

Mandhane, J. M., G. A. Gregory, and K. Aziz, "A Flow Pattern Map for Gas-Liquid Flow in Horizontal Pipes," *Intern. J. Multiphase Flow*, **1**, 537-553 (1974).

Sakaguchi, T., K. Akagawa, and H. Hamaguchi, "Transient Behavior of Air-Water Two-Phase Flow in a Horizontal Tube," ASME Paper 73-WA/HT-21, Winter Annual Meeting, Detroit, Mich. (Nov., 1973).

Schicht, H. H., "Flow Pattern for an Adiabatic Two-Phase Flow of Water and Air Within a Horizontal Tube," *Verfahrenstechnik*, 3, 153 (1969).

Sternling, C. V., "Two Phase Flow—Theory and Engineering Decision," Institute Lecture presented at AIChE Annual Meeting, Philadelphia, Pa. (Dec., 1965).

Stoker, J. J., *Water Waves*, Interscience, New York (1957).

Taitel, Y., and A. E. Dukler, "A Model for Predicting Flow Regime Transitions in Horizontal and Near Horizontal Gas-Liquid Flow," *AIChE J.*, **22**, No. 3, 47-55 (1976).

———, "A Model for Slug Frequency During Gas-Liquid Flow in Horizontal and Near Horizontal Pipes," *Intern. Multiphase Flow*, 3, 585 (1977).

APPENDIX: SEQUENCE FLOW RATE CONTROL SYSTEM

Commercial flow control valves have only limited rangeability, with the ratio of maximum to minimum flow rate seldom exceeding 50. If flow rates must be varied over a wider range than 50 in a single experiment, then sequencing valving can be used. In this technique, flow takes place first through the smaller valve, and then, at the appropriate control point, the larger valve opens and high flow rates are accommodated by increased opening of this large valve. This need for a wide range of rates and thus for sequencing introduces two problems: the selection of valves must be such as to insure a smooth transition as the second valve opens, and flow rate transducers must usually be paralleled and with different ranges to insure accuracy both at low and high flow rates.

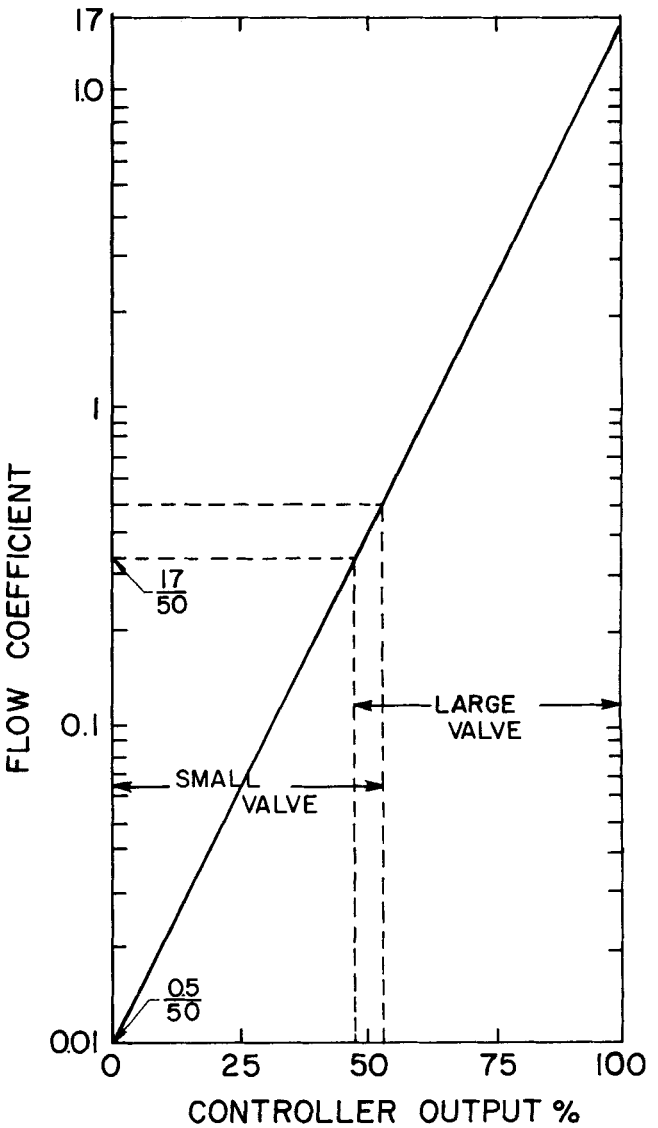

Fig. A-1. Operating range of sequenced equal percentage valves.

Sequencing of Valves

Equal percentage stem Foxboro control valves were used in these experiments with rangeability of 50. Figure A1 shows the flow coefficient (which is directly proportional to flow rate) of these valves. The maximum coefficient of the largest valve at full opening was 17, and its minimum value at 17/50 = 0.34. The second valve was selected which had a maximum coefficient of 0.50 and thus a minimum one of 0.01. Thus, the rangeability of the two valve system is 1 700.

In deciding how to adjust the control signal, the variation of the coefficient with controller output must be examined. Figure A1 presents this information for the Foxboro system. The controller produces a pneumatic signal of 3 to 15 lb/in.²*

* Equivalence in SI units is 0.2067 × 10^5 to 1.0339 × 10^5 Newtons/m².

in proportion to its output. Thus, in this case switch over is set at 50% or at 9 lb/in.². The large valve diaphragm is set to be closed below 9 lb/in.², to start opening at 9 lb/in.², and to be full open at 15 lb/in.². The small valve opens at 3 lb/in.² and is full open at 9 lb/in.².

The hookup to make this possible is shown in Figure A2. The controller pressure signal is branched through three way solenoid valves to the diaphragms of the control valves. At

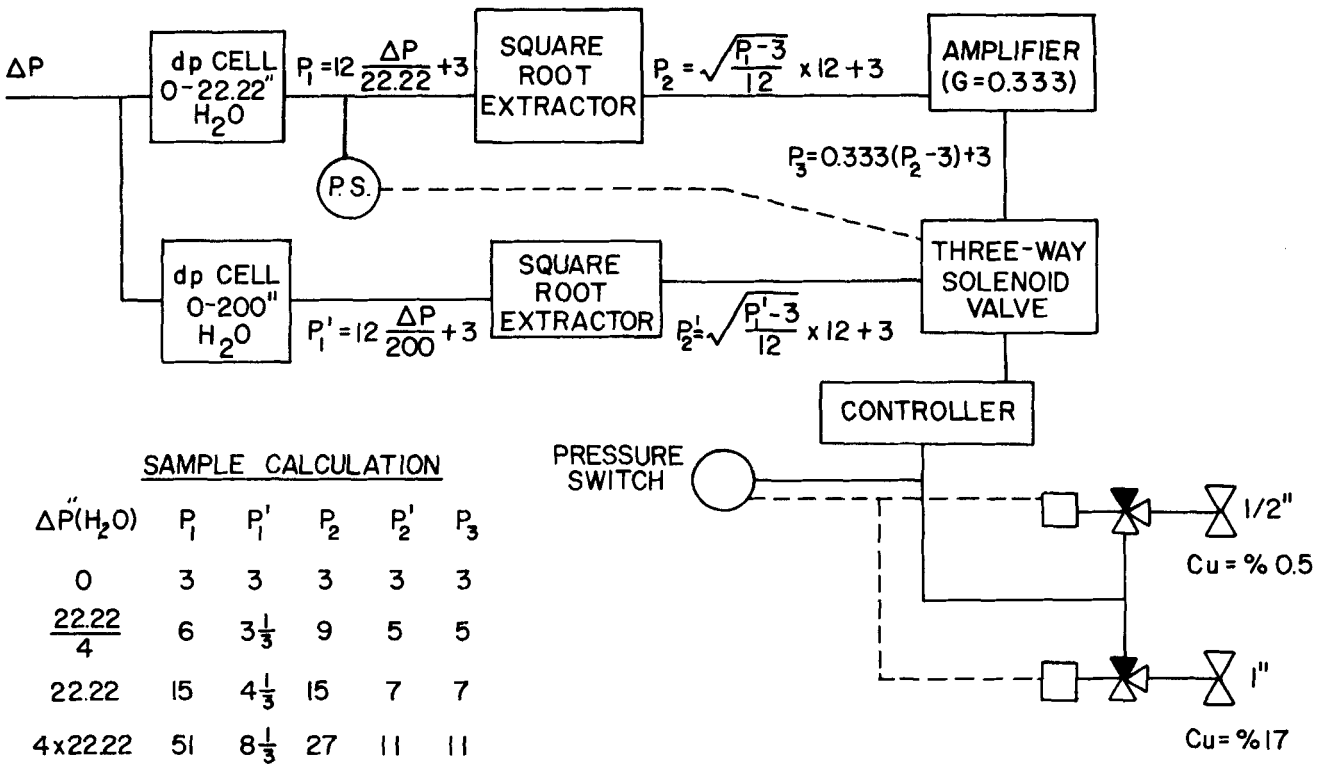

SAMPLE CALCULATION

$\Delta P''(H_2O)$	P_1	P_1'	P_2	P_2'	P_3
0	3	3	3	3	3
22.22/4	6	$3\frac{1}{3}$	9	5	5
22.22	15	$4\frac{1}{3}$	15	7	7
4x22.22	51	$8\frac{1}{3}$	27	11	11

Fig. A-2. Switching system for sequence valving.

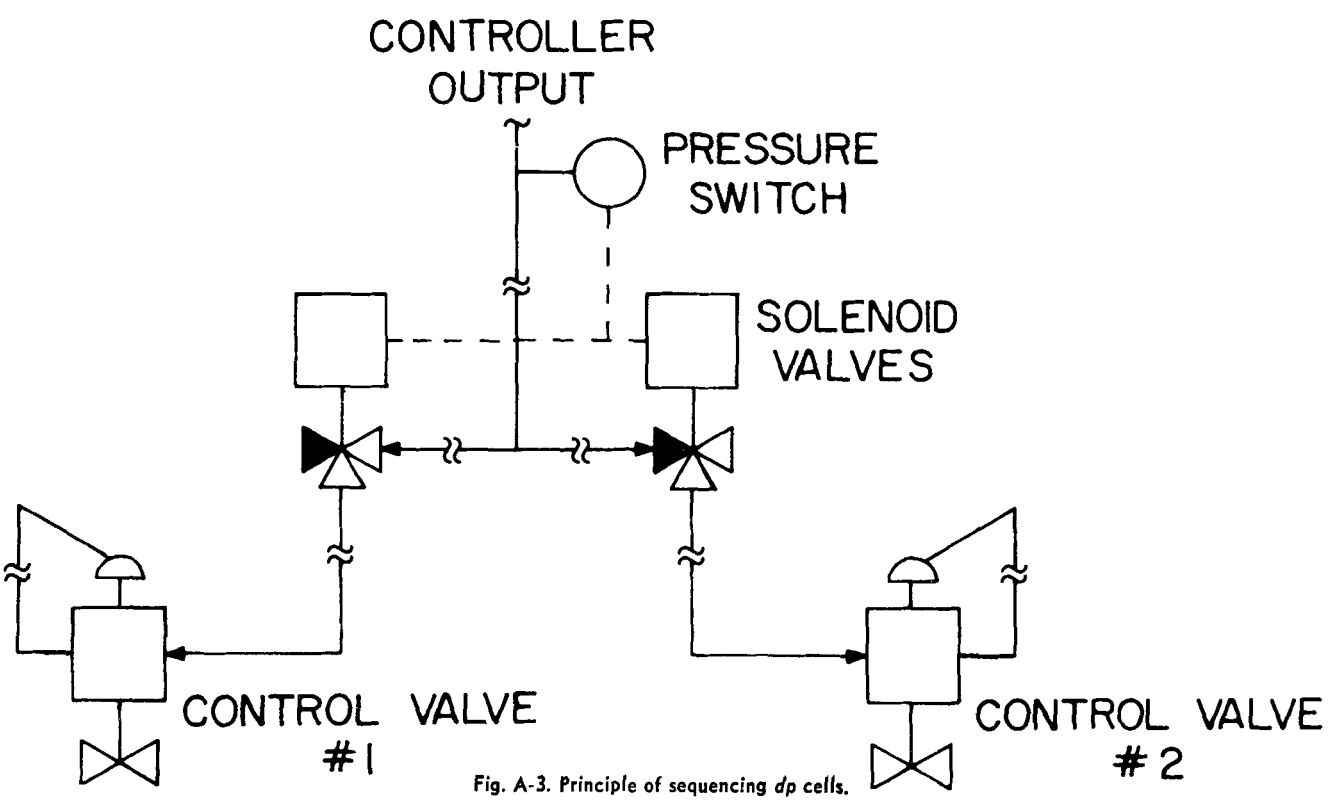

Fig. A-3. Principle of sequencing *dp* cells.

signal pressures below 9 lb/in.^{2}, both solenoids are passive. With the hookup shown, valve No. 1 receives signal and valve No. 2 is vented. When the signal reaches 9 lb/in.^{2}, the pressure switch activates the solenoids. The pressure on the diaphragm of valve No. 1 is vented to atmosphere, and the signal is directed to the diaphragm of valve No. 2. When the diaphragms on these valves are vented, the valves are closed.

Sequencing of Flow Transducers

Flow rates were measured with a single orifice plate and orifice flanges with differential pressure (d/p) cells used to detect pressure difference. Since the accuracy of such cells is related to the maximum reading, it was necessary to use two cells to insure the required accuracy at low flow rates. Standard Foxboro d/p cells were selected with maximum pressure differentials of 200 in. water and 22.22 in. water.

Figure A3 shows the sequencing system. Both cells continuously measure the differential pressure, but a three-way solenoid valve is used to switch the signal from the d/p cells to the controller, depending on the magnitude of the pressure difference. Square-root extractors are used to process the signal from the d/p cells to provide a flow signal to the controller linear with flow. Sample calculations showing the operation of the system are included in the table to demonstrate that smooth switch over will take place.

Manuscript received November 18, 1977; revision received May 10, and accepted June 22, 1978.